Efflux pumps mediate changes to fundamental bacterial physiology via membrane potential

Emily E Whittle[1], Oluwatosin Orababa[1†], Sarah J Element[1], Jessica MA Blair[1]* and Tim W Overton[2]*

[1] Institute of Microbiology and Infection, College of Medical and Dental Sciences and [2]School of Chemical Engineering, University of Birmingham, Edgbaston, Birmingham, B15 2TT, UK

† Present address: School of Life Sciences, The University of Warwick, Coventry, CV4 7AL

* To whom correspondence should be addressed:

Jessica MA Blair: j.m.a.blair@bham.ac.uk

Tim W Overton: t.w.overton@bham.ac.uk

Abstract

Efflux pumps are well known to be an important mechanism for removing noxious substances such as antibiotics from bacteria. Given that many antibiotics function by accumulating inside bacteria, efflux pumps contribute to resistance. Inactivation of efflux pumps is a potential strategy to combat antimicrobial resistance, as bacteria would not be able to pump out antibiotics. We recently discovered that the impact of loss of efflux function is only apparent in actively growing cells. We demonstrated that the global transcriptome of *Salmonella enterica* serovar Typhimurium is drastically altered during slower growth leading to stationary phase cells having a re-modelled, less permeable, envelope that prevents antibiotics entering the cell. Here, we investigated the effects of knocking out the major efflux pump of *Salmonella* Typhimurium, AcrB, on global gene transcription across growth. We revealed that an *acrB* knockout entered stationary phase later than the wild type strain SL1344, and displayed increased and prolonged expression of genes responsible for anaerobic energy metabolism. We devised a model linking efflux and membrane potential, whereby deactivation of AcrB prevents influx of protons across the inner membrane and thereby hyperpolarisation. Knockout or deactivation of AcrB was demonstrated to increase membrane potential. We propose that the global transcription regulator ArcBA senses changes to the redox state of the quinol pool (linked to the membrane potential of the bacterium) and coordinates the shift from exponential to stationary phase via the key master regulators RpoS, Rsd, and Rmf.

Inactivation of efflux pumps therefore influences the fundamental physiology of *Salmonella*, with likely impacts on multiple phenotypes.

Importance

We demonstrate for the first time that deactivation of efflux pumps brings about changes to gross bacterial physiology and metabolism. Rather than simply being a response to noxious substances, efflux pumps appear to play a key role in maintenance of membrane potential and thereby energy metabolism. This discovery suggests that efflux pump inhibition or inactivation might have unforeseen positive consequences on antibiotic activity. Given that stationary phase bacteria are more resistant to antibiotic uptake, late entry into stationary phase would prolong antibiotic accumulation by bacteria. Furthermore, membrane hyperpolarisation could result in increased generation of reactive species proposed to be important for the activity of some antibiotics. Finally, changes in gross physiology could also explain the decreased virulence of efflux mutants.

Keywords

Hyperpolarisation, RND efflux pump, AcrAB-TolC, ArcBA, redox state, energy metabolism.

Introduction

Many antibiotics function by accumulating inside bacteria and inhibiting essential metabolic functions such as protein synthesis, DNA repair, or cell wall synthesis (1). Bacteria can therefore protect themselves against these antibiotics by decreasing intracellular accumulation. There are two main mechanisms for this: removal of antibiotics from inside the cell via efflux pumps (2); and prevention of influx of antibiotics across the envelope (3). The major efflux pump in *S*. Typhimurium is AcrAB-TolC, a member of the RND family (4) comprising the transporter AcrB, the periplasmic adaptor protein AcrA, and the outer membrane channel TolC. AcrAB-TolC has been shown to have a wide substrate range and mediate resistance to multiple antibiotics. Loss of AcrB function through mutation or inhibition has been shown to make *S*. Typhimurium hyper-susceptible to antibiotics as well as avirulent, unable to form biofilm and less motile (5, 6); major changes to the physiology of the organism.

In an attempt to understand the physiological consequences of loss of efflux function previous studies have compared global gene expression in the *S.* Typhimurium wild type and efflux mutants

62 (5–7). Wang-Kan *et al*. compared an *acrB* D408A mutant (defective in AcrB efflux function) with the
63 wild type *S.* Typhimurium SL1344, both in exponential phase growth in MOPS minimal medium (6)
64 and stationary phase growth in rich LB broth (7). The latter study also compared gene expression in
65 *E. coli* K-12 MG1655 and its *acrB* D408A mutant, and characterised the exometabolome and
66 endometabolome of each of the four strains in order to better understand the substrates of the
67 AcrAB-TolC pump. The effect of deletion of *acrD*, encoding an alternative efflux pump with narrower
68 substrate specificity to AcrB, on global gene expression has also been characterised (8). However,
69 each of these studies compared gene expression at a single timepoint.

70 In a previous study (9) we investigated the dynamic balance between efflux and prevention of influx
71 of antibiotics across the Gram-negative bacteria and revealed that efflux is more important during
72 rapid exponential phase growth as the envelope is more fluid and antibiotics can pass into the
73 bacterium more readily. However, in stationary phase, the envelope is remodelled and becomes less
74 amenable to antibiotic entry, thus preventing intracellular accumulation, meaning that efflux has
75 less impact. We used RNA-Seq in *Salmonella* Typhimurium SL1344 to map global gene expression as
76 bacteria transitioned from exponential to stationary phase, highlighting gene expression changes
77 potentially responsible for remodelling multiple layers of the envelope. Work by others has also
78 revealed that prevention of influx and active efflux have different relative contributions during
79 antimicrobial resistance development across Gram-negative pathogens (10, 11).

80 Given that the relative impact of efflux varies during bacterial growth, in the present study, we
81 tracked gene expression at 1, 3 and 5 hours growth in the wild type and an Δ*acrB* mutant to enable
82 the dynamics of gene expression to be compared. We sought to better understand the physiological
83 changes brought about by deletion of *acrB*, and to differentiate between the direct effects of AcrB as
84 an efflux pump (eg removal of compounds from the bacterium) and the secondary effects brought
85 about by the deletion.

86 We show that deletion of *acrB* has wide-ranging effects on physiology and we propose and test a
87 model that links efflux, membrane potential, redox state of the cell, and entry into stationary phase.
88 This suggests that efflux pumps are deeply embedded in bacterial physiology, and loss of AcrB
89 function perturbs the transition from exponential phase to stationary phase physiology. We also
90 demonstrate the benefits of transcriptome analysis across growth, using samples taken at multiple
91 timepoints, to discover novel aspects of gene regulation and physiology.

92

93

Results

We previously published the results of a transcriptome analysis showing transition of the wild type *S.* Typhimurium strain SL1344 from exponential to stationary phase (9). Samples were taken after 1, 3, and 5 hours growth in MOPS minimal medium, and gene expression was tracked using RNA-Seq across growth. This study revealed changes to aspects of physiology as bacteria transitioned from the rapid growth of exponential phase to the slower growth of stationary phase. We specifically focused on changes in gene expression responsible for remodelling the bacterial envelope from a relatively permeable structure in rapid growth to a far less permeable state in stationary phase. This decreased envelope permeability is likely a key contributor to why stationary phase bacteria are more resistant to multiple antibiotics (12, 13) as well as other stressors (14, 15).

In the present work, we expanded this study by repeating these transcriptomics experiments in an *S.* Typhimurium Δ*acrB* mutant (9), similarly taking samples after 1, 3, and 5 hours growth in MOPS minimal medium. The two strains grew similarly under these conditions. First, we compared how changes in gene expression over time differed between the wild type and Δ*acrB* strains. Gene expression was compared between 1 h and 3 h, 1 h and 5 h, and 3 h and 5 h timepoints for each strain (Figure 1). This revealed that more genes were differentially regulated early in growth (the 1 h vs 3 h comparison) in the wild type than in the Δ*acrB* mutant. Comparing later timepoints, there are more differentially expressed genes for the 3 h vs 5 h comparison in the Δ*acrB* mutant than the wild type. This suggests that changes in gene expression occur later in the Δ*acrB* mutant than the wild type.

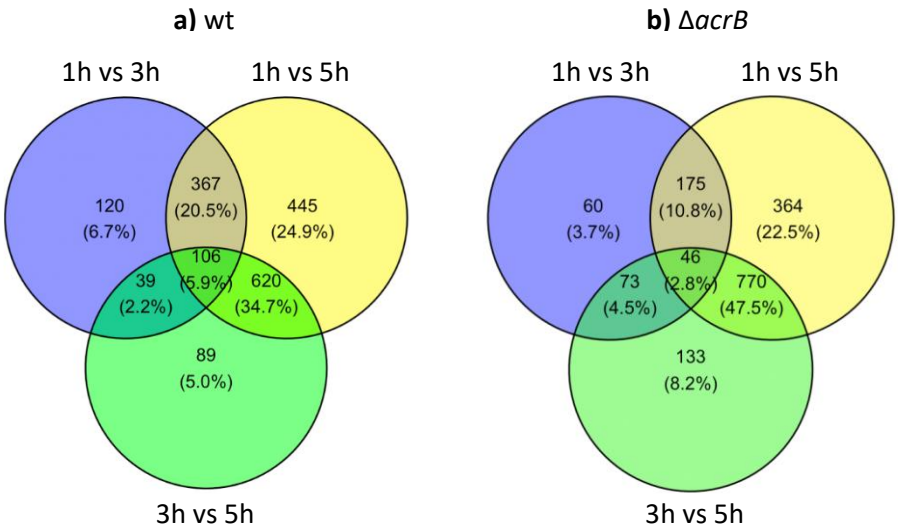

Figure 1. Venn diagrams comparing gene expression in the (a) wild type and (b) Δ*acrB* strain. Number of genes differentially expressed ($\log_2$ foldchange ≥ 1.5 and $p_{adj} < 0.05$) for each comparison is shown.

117 We wanted to understand why expression of more genes changed between 1 h and 3 h in the wild
118 type than in the Δ*acrB* strain, and the effect this would have on physiology. We classified genes into
119 three groups (Figure 2) based on their log_2 fold change (log_2FC) from 1 h to 3 h in each strain, and
120 their Δlog_2FC value, calculated by subtracting the Δ*acrB* log_2FC from the wild type log_2FC. A positive
121 Δlog_2FC value denotes a gene that is more upregulated or less downregulated in the Δ*acrB* strain
122 than the wild type. Genes with a negative Δlog_2FC value are more upregulated or less downregulated
123 in the wild type.

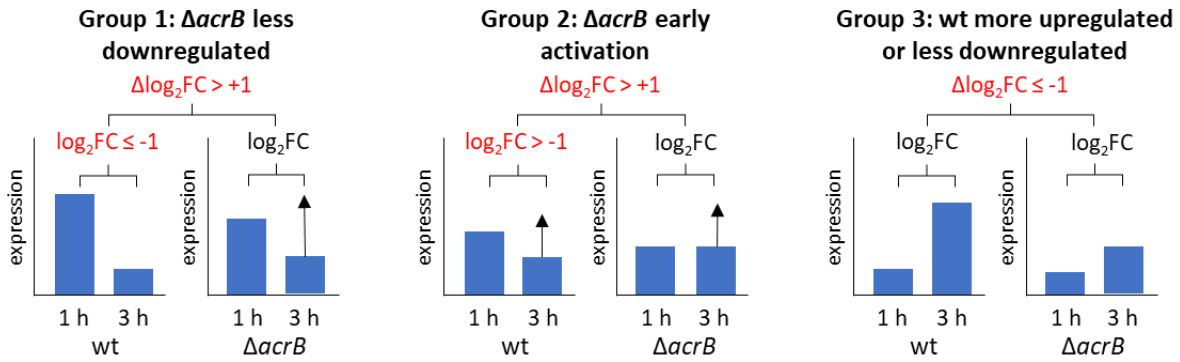

124

125 **Figure 2. Data analysis strategy to characterise differentially expressed genes.** For each gene, transcript levels
126 at 1 h and 3 h were compared and a log_2 fold-change (log_2FC) value calculated. The log_2 fold-change for the
127 Δ*acrB* mutant was subtracted from the wt log_2FC to give a Δlog_2FCvalue indicating the difference in regulation
128 between the two strains. A positive Δlog_2 value indicates a gene is more upregulated or less downregulated in
129 Δ*acrB* for the 1 h vs 3 h timepoints. A negative Δlog_2 value indicates that a gene is more upregulated or less
130 downregulated in the wild type.

131

132 Group 1 comprises genes that were downregulated from 1 h to 3 h in the WT ($log_2FC \leq -1$) and less
133 downregulated in the Δ*acrB* strain, thereby having a Δlog_2FC of ≥ 1. Group 2 contains genes that
134 were not downregulated from 1 h to 3 h in the wt ($log_2FC > -1$) but had a Δlog_2FC of ≥ 1, thereby
135 were more upregulated or less downregulated in the Δ*acrB* mutant. Group 3 contains genes that
136 were more upregulated from 1 h to 3 h in the wild type than in the Δ*acrB* mutant. Genes with a
137 $p_{adj} > 0.05$ (non-significant) for the 1 h to 3 h timepoints in either wt or Δ*acrB* were omitted from this
138 analysis.

139 ***Group one – late repression in the ΔacrB strain***

140 The 166 genes in group one are more downregulated between 1 h and 3 h in the wild type than the
141 Δ*acrB* strain (Supplemental Table S1). The largest categories of genes in this group are those
142 encoding tRNAs (34 genes) and ribosomal proteins and other proteins involved in translation (33
143 genes). Many of these genes (including the tRNA genes) are known to be downregulated during the
144 entry into stationary phase by the stringent response, mediated by ppGpp (16). For many of these

145 genes, expression is downregulated in the wild type from 1 h to 3 h and then does not change
146 significantly from 3 h to 5 h, whereas in the Δ*acrB* strain expression does not change from 1 h to 3 h
147 but decreases from 3 h to 5 h. This suggests that the Δ*acrB* strain enters stationary phase later than
148 the wild type SL1344 strain.

149 Fifteen genes in this group are involved in envelope functions including inner membrane protein
150 insertion, outer membrane lipoprotein trafficking, LPS and lipid A synthesis, and peptidoglycan
151 synthesis and remodelling. The peptidoglycan-related genes *ldtB*, *mrcA* and *pbpG* are implicated in
152 exponential phase functions (9, 17). Five genes involved in nucleotide metabolism and 6 genes in
153 amino acid metabolism, also important during rapid growth, are also in this group, reinforcing the
154 idea that stationary phase transition is delayed in the Δ*acrB* strain.

155 Four genes in group one are related to polyamines, specifically putrescine import and spermidine
156 synthesis. Recently, the efflux regulator AcrR (which represses expression of *acrAB*) was shown to
157 bind to three polyamines and regulate aspects of polyamine efflux and metabolism in *E. coli* (18).
158 Seven genes of *Salmonella* pathogenicity island 1 (SPI-1), encoding a type III secretion system
159 required for invasion of epithelial cells, are in group one. The SPI-1 regulatory network is very
160 complex (19) and comprises transcription factors encoded both within and outside SPI-1. Expression
161 of SPI-1 is bistable (20) and is influenced by multiple environmental stimuli including osmolarity,
162 oxygen tension, bile, [Mg^{2+}], and pH. Two genes in SPI-11, implicated in survival in the macrophage
163 (21), are also in group one. Alteration in SPI expression would likely influence virulence, which is
164 known to be decreased upon loss of AcrB function (6).

165 Other transcriptomic studies identified genes in group one being as being differentially regulated in
166 the *S.* Typhimurium wild type and strains lacking *acrB* or *acrB* function (*acrB* D408A mutant).
167 Comparison in exponential phase in MOPS minimal medium (5, 6) revealed that SPI-1 genes were
168 downregulated in an *acrB* knockout mutant and in the *acrB* D408A mutant. In stationary phase (7),
169 rRNAs, tRNAs, SPI-11 and some SPI-1 genes were downregulated (although the SPI-1 *sipABCD* TTSS
170 genes, not members of groups one - three in the present study, were upregulated in the mutant).
171 However, our data suggests that this is a response to fundamental changes in physiology brought
172 about by deletion of *acrB*, and not necessarily direct regulation of pathogenicity islands.

173 ***Group two – early activation in the ΔacrB strain***

174 The 46 genes in group two (Supplemental table S2) are more upregulated between 1 h and 3 h in the
175 *acrB* strain than in the same time period in the wild type, so are classified as "early activation". On
176 initial inspection, this group contains many genes known to be anaerobically activated. For each
177 gene, expression data in the gene expression database SalComMac (22, 23) was consulted to identify
178 which genes are anaerobically activated; in this database, "anaerobic shock" is classified as aerobic
179 growth followed by 30 minutes in a sealed static tube (22). It should be noted that the SalComMac
180 data is for *S*. Typhimurium strain 4/74; SL1344 is a *hisG* auxotroph of 4/74 (24), although we believe
181 that data should be broadly comparable for the two strains.

182 Many of the anaerobically-activated genes are activated by the oxygen-sensing global regulator FNR
183 in *Salmonella* (25) and / or *E. coli* (26). These include genes encoding the periplasmic nitrate and
184 nitrite reductases responsible for anaerobic respiration at low NO_2^- and NO_3^- concentrations (27, 28),
185 the anaerobic serine/threonine degradation enzyme TdcB that is suggested to be critical for energy
186 metabolism during changes in oxygen tension (29), and the two cytochrome *c* maturation (Ccm)
187 operons, one of which is downstream of the *nap* operon (30). The cytochrome *c* peroxidase *yhjA*/*ccp*
188 is also in this group, which has been shown to be FNR-activated (25) and enables respiratory growth
189 on peroxide (31). The *ccp* gene is upstream of the second *ccm* cluster and may form a single operon.
190 RS22105, annotated as a molybdopterin-dependent oxidoreductase and proposed to be a DMSO
191 reductase distinct from DmsABC, has been shown to be FNR activated in *Salmonella* (25), as has
192 *yhbU/ubiU* which encodes part of the oxygen-independent ubiquinone synthesis pathway (32).

193 A high affinity nickel uptake system (*yntABCDE/nikABCDE*) is in the grouping (33); these genes are
194 FNR activated in *E. coli* although were not identified in the *Salmonella* FNR study (25). In *E. coli*,
195 *nikABCDE* expression is linked to that of the Ni^{2+} cofactor-containing hydrogenases required for
196 respiration of fumarate and formate (34). RS15890 and RS15900 (*ecfT*) are two members of a
197 putative 5-gene operon encoding an ECF transporter suggested to import Co^{2+} (35) that is conserved
198 in pathogenic *E. coli* strains. SalComMac data suggests that this operon is anaerobically activated.

199 The remaining anaerobically-activated genes in this group are of unknown function or are poorly
200 characterised: *yecH* has been shown to be downregulated by adrenaline (36); *ompX* is in SPI-5 (37)
201 and has been found to be overexpressed in a *dksA* mutant (38); two LysR family transcriptional
202 regulators (RS11710 and RS19740); a putative transketolase RS12010; and hypothetical protein
203 RS12010.

204 It should be noted that for many of these anaerobic genes, expression increases from 1 h to 3 h and
205 then decreases from 3 h and to 5 h. The magnitude of the increase in expression is larger in the *acrB*
206 strain. Taken together, genes in this group enable anaerobic energy generation through respiratory
207 and substrate-level routes.

208 As well as the anaerobically-activated genes in this group, there are also several genes that are
209 anaerobically repressed in SalComMac, including the tyrosine importer *tyrP*, the flagellar genes *fliR*,
210 *fliF* and *fliH* and the proposed virulence factor *srfA* which was also identified as a class 2 flagellar
211 gene (39) whose expression is activated by the flagellar master regulator FlhDC. As previously noted,
212 loss of AcrB function reduces *Salmonella* motility (5). A link between motility and SPI-1 has also been
213 reported (40).

214 In previous transcriptomic studies, Wang-Kan et al (6) identified anaerobically-activated genes
215 including nitrate and nitrite reductase and flagellar genes being upregulated in the *acrB* D408A
216 mutant in exponential phase. In stationary phase, some anaerobically-relevant and flagellar genes
217 were also upregulated (7).

218 ***Group three – late activation in the ΔacrB strain***

219 Group three comprises 53 genes that are more activated in the wild type than in Δ*acrB* at three
220 hours, so the opposite pattern to genes in groups one and two (Supplemental Table S3). The most
221 striking group of genes in this group are the *met* genes involved in methionine biosynthesis from
222 aspartate, methionine uptake, and S-adenosyl methionine (SAM) biosynthesis; expression of these
223 genes is seen to "spike" at 3 h in the wt, with upregulation at 3 h vs 1 h and downregulation at 5 h vs
224 3 h. In the Δ*acrB* strain these genes are less upregulated at 3 h and many are further upregulated at
225 5 h, indicating much later induction. In *E. coli* these genes are all repressed by the regulator MetJ
226 which binds to methionine and SAM (41). Our data suggest that these routes to SAM are highly
227 upregulated on entry to stationary phase. SAM is an essential metabolite and a major methyl donor
228 for protein and DNA methylation and polyamine synthesis; in the transition to stationary phase, SAM
229 is also a methyl donor for cyclopropane fatty acid synthesis (42). In *E. coli*, the SAM synthase *metK* is
230 essential (43) and depletion of SAM using a *metK84* mutant leads to a cell division defect (44). In *S*.
231 Typhimurium, methionine biosynthesis or import are required for infection in mice and methionine
232 was implicated in aspects of peptidoglycan synthesis (45).

233 These data suggest that the methionine and / or SAM pool in the wild type is depleted at 3 h growth,
234 and these pathways are upregulated to replenish the pool. The transcriptomics data in SalComMac
235 shows that most of the *met* genes are not upregulated in stationary phase, although that dataset

236 was generated for cultures grown in rich Lennox broth (22). We suggest that in Lennox broth,
237 methionine is available (around 70 mg/L based on typical composition values (46)) so can be readily
238 imported and converted to SAM, whereas in MOPS minimal medium used here, methionine needs
239 to be synthesised from aspartate, hence activation of the *met* genes. This suggests that methionine
240 could be a growth limiting nutrient in these conditions.

241 A cluster of genes (*ybdL, ybdH, ybdD, ybdM*) are also regulated in a similar manner to the *met* genes.
242 *E. coli* YbdL has methionine aminotransferase activity (47) and is believed to be involved in
243 methionine recycling following polyamine synthesis (48). YbdH is annotated as a putative glycerol
244 dehydrogenase and the homologue in *E. coli* has been identified as a hydroxycarboxylate
245 dehydrogenase (49). The *E. coli ybdD* homologue has been identified (with CstA) as part of a
246 pyruvate import system (50) and *ybdM* has been identified as a transcriptional regulator related to
247 SpoOJ (51). A predicted MetJ binding site in this cluster could explain its regulation (41).

248 The PstSCAB high-affinity phosphate importer is poorly understood in *Salmonella* but is known to be
249 induced in *E. coli* in response to phosphate limitation, and is activated by RpoS (52). ProP is
250 responsible for the uptake of osmoprotectants proline and glycine betaine; expression in *E. coli* is
251 induced by RpoS and Fis on entry to stationary phase (53). Expression of *mysB*, *yahO,* and *yceK* are
252 also RpoS-induced (54). Expression of *katG* in *E. coli* was also shown to increase on entry into
253 stationary phase, although in an RpoS-independent manner (55).

254 Two genes with key roles in regulating entry into stationary phase entry in this group: *rsd* encodes an
255 anti-sigma factor that deactivates the exponential phase housekeeping sigma factor σ^{70} RpoD (56);
256 and *rmf* induces ribosome dimerization and hibernation (57). Expression of *rmf* is highly upregulated
257 in stationary phase in the SalComMac dataset (22). Both of these genes are upregulated far later in
258 the *acrB* mutant than in the wild type in our dataset; together with the other stationary-phase
259 induced genes in group three, this supports the later onset of stationary phase in Δ*acrB* than the
260 wild type.

261 Expression of *aceB* is regulated by multiple transcription factors in *E. coli*, including ArcA (58). There
262 are also a number of genes in SPI-2, involved in intracellular survival, and chemotaxis-related genes
263 in group three.

264 Lower expression of SPI-2 genes were observed in other transcriptomics studies in the *acrB* D408A
265 mutant in exponential (6) and stationary phase (7), although the *met* genes and many others in
266 group three were not reflected in the datasets of previous studies. The reason for this is likely
267 because most genes in this group were transiently expressed in the wild type; we observed a "spike"

268 of expression, and later expression in the Δ*acrB* mutant. This reveals a key advantage of our
269 approach; such a "spike" could be missed if only a single timepoint was used to measure
270 transcriptomes. Taking samples through growth allows the expression of each gene to be tracked
271 and the profiles of gene expression over time to be compared.

272 ***A model linking efflux and stationary phase via membrane potential***

273 Previous studies have proposed that changes in gene expression and physiology in efflux knockouts
274 have been caused by the lack of efflux of a signalling molecule (for example an autoinducer), giving
275 rise to changes in intracellular and/or extracellular concentrations of that molecule and a resultant
276 change in gene regulation and physiology. However, we realised that knockout of *acrB* could trigger
277 an alternative signalling cascade. As AcrB requires proton motive force (PMF) for function,
278 deactivation of AcrB would decrease of influx of protons across the inner membrane, resulting in
279 membrane hyperpolarisation and thus alter the redox state of the cell. This has been built into a
280 model (Figure 3) whereby the membrane potential and redox state of the bacterium plays a key role
281 in the transition from exponential to stationary phase, mediated by the two-component ArcBA
282 system (59). Deletion of AcrB results in perturbation of the membrane potential and thereby the
283 redox balance of the cell and thus disrupts this regulation, resulting in a) late entry into stationary
284 phase and b) upregulation of anaerobic energy metabolism pathways.

285 The global regulator ArcBA regulates gene expression on the shift from aerobic to anaerobic
286 metabolism (59) and is also thought to play a role in response to other stresses such as reactive
287 oxygen species (ROS) and during infection in *Salmonella* (60, 61). Knockouts of *arcA* and *arcB* in *S.*
288 Typhimurium reduce intracellular survival in epithelial cells, macrophages and neutrophils, and are
289 attenuated in a mouse model (60). The ArcBA regulon has been characterised in *E. coli* (reviewed by
290 (59)) and *Salmonella* both aerobically and anaerobically (61, 62). The sensor kinase ArcB
291 autophosphorylates itself and then phosphorylates the response regulator ArcA; phospho-ArcA
292 binds promoter DNA and regulates gene expression (Figure 3a). Oxidised quinones repress the
293 kinase activity of ArcB (63) thus ArcBA is a direct sensor of the quinol pool redox state. Highly
294 oxidised quinone (Q) leads to low ArcA activity whereas highly reduced quinol (QH_2) leads to high
295 ArcA activity.

296 ArcA has previously been shown to repress expression of *rpoS*, *rsd*, and *rmf*, three genes that
297 mediate important aspects of the switch from exponential phase to stationary phase (14, 64). RpoS
298 is the sigma factor that is dominant in stationary phase (14); *rpoS* transcription is repressed by ArcA
299 in *E. coli* (65) and *Salmonella* (66). In addition, activated ArcB phosphorylates RssB, which targets
300 RpoS protein for degradation by the ClpXP protease (65). ArcAB-RssB therefore acts as a key

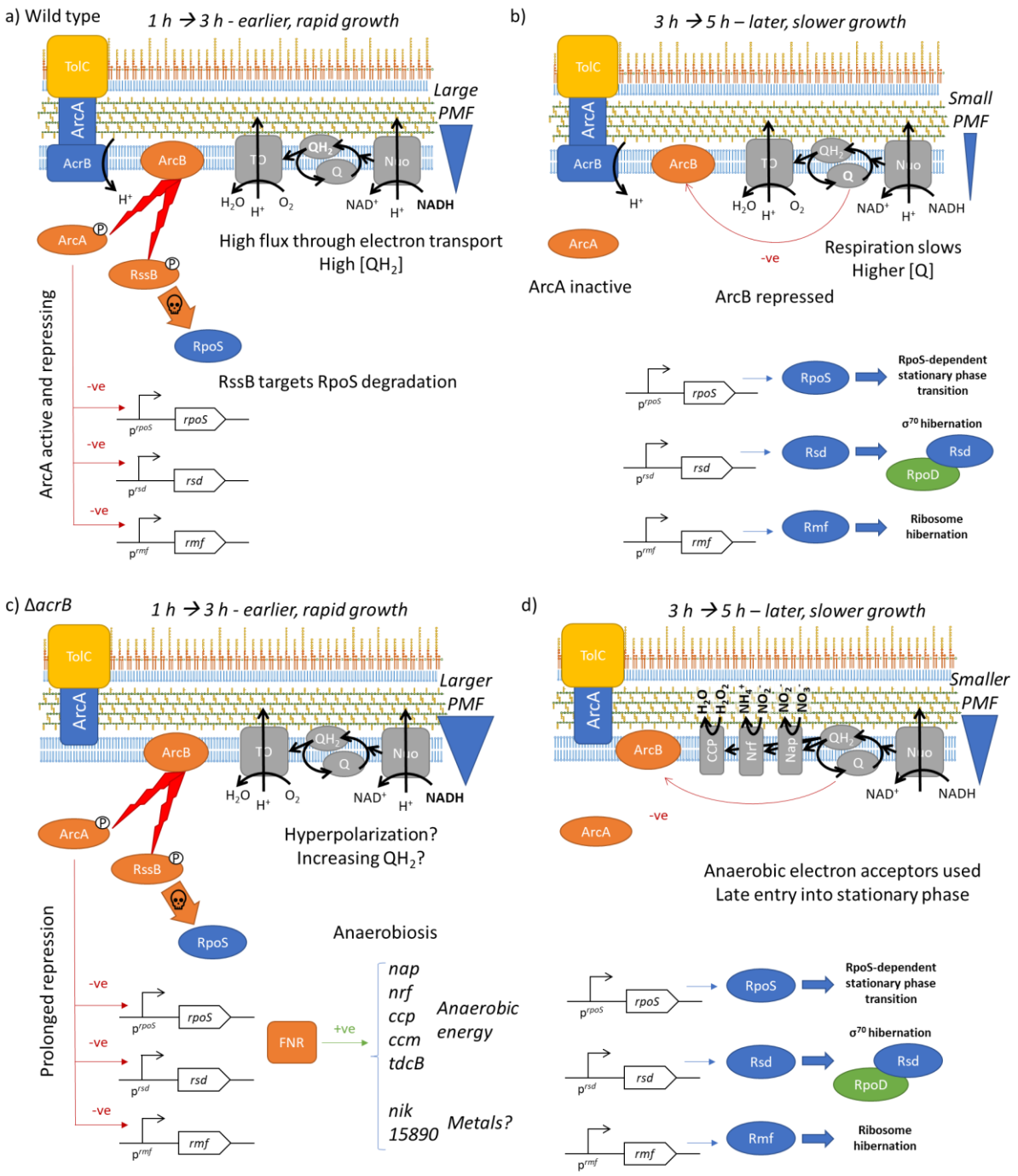

Figure 3. Model of the mechanism of ArcBA-mediated redox control of stationary phase entry and the impact of an AcrB mutant. In the wild type strain during rapid growth (a), high flux through the electron transport chain results in a reduced quinol pool (QH_2) which permits ArcBA to be active, repressing expression of *rpoS*, *rsd* and *rmf*. RssB also targets RpoS protein for degradation. As growth slows (b), the quinol pool becomes more oxidised (Q), deactivating ArcB, permitting activation of *rpoS*, *rsd* and *rmf*, triggering entry into stationary phase. In a *ΔacrB* mutant (c), proton motive force is higher for longer during growth, repressing *rpoS*, *rsd* and *rmf* and delaying entry into stationary phase. As a result, exponential phase physiology is extended (d), necessitating upregulation of genes involved in anaerobic energy metabolism (Nap, Nrf and CCP shown), likely via the global regulator FNR. TO: Terminal oxidases.

312 gatekeeper to entry into stationary phase. Rsd is an anti-sigma factor that deactivates the
313 exponential phase housekeeping sigma factor σ^{70} / RpoD (56). Expression of *rsd* is regulated by ArcA
314 in both *E. coli* (67) and *Salmonella* (61). Rmf induces ribosome dimerization and hibernation in
315 stationary phase (57); its expression is ArcA-regulated in *Salmonella* (61) and *E. coli* (64).

316 In the wild type in rapid growth, relatively high flux through electron transport to oxygen results in a
317 highly reduced quninol pool (QH_2). This would enable ArcBA to be active, repressing *rpoS*, *rsd* and
318 *rmf*. During entry into stationary phase, the quinol pool becomes more oxidised, de-activating ArcBA
319 and thus permitting *rpoS*, *rsd* and *rmf* expression and activity. In the transition of the *ΔacrB* strain to
320 stationary phase, the inner membrane would become hyperpolarised; this would alter the redox
321 state of the quinol pool, meaning that ArcBA remains active and RpoS, Rsd and Rmf activities are
322 repressed for longer during growth. This would delay onset of stationary phase in the Δ*acrB* mutant.
323 The genes *rsd* and *rmf* both fall into group three; Table 1 summarises their expression data.
324 Expression of *rpoS* is insignificant ($p_{adj} > 0.05$) in the wild type between 1 h and 3 h, although
325 downregulated between 1 h and 3 h in the Δ*acrB* mutant.

326

Log₂ fold change				**Δ*acrB* – wt Δlog₂**				
wt 1vs3	**wt 3vs5**	**acrB 1vs3**	**acrB 3vs5**	**1vs3**	**3vs5**	**ID**	**Gene**	**STM**
0.98	0.35†	-0.69	1.59	-1.67	1.24	SL1344_RS21380	*rsd*	STM4165
0.36†	0.73†	-1.17	2.19	-1.53	1.46	SL1344_RS15130	*rpoS*	STM2924
2.30	3.74	1.05	4.61	-1.25	0.87	SL1344_RS05235	*rmf*	STM1066

327

328 **Table 1. Gene expression data for the key stationary phase regulators *rsd*, *rmf*, and *rpoS*.** Log_2 fold change values for each
329 gene: 1 h vs 3 h in the wild type; 3 h vs 5 h in the wild type; 1 h vs 3 h in Δ*acrB*; 3 h vs 5 h in Δ*acrB*. ΔLog_2 values for the 1 h
330 vs 3 h and 3 h vs 5 h comparisons. Δlog_2 values are calculated by Log_2 fold change for Δ*acrB* minus Log_2 fold change for the
331 wild type. ID: locus name. Fold changes that are insignificant ($p_{adj} > 0.05$) are marked with a dagger †. Other fold changes
332 are colour coded as in Supplemental tables.

333 In the absence of a transition into stationary phase, exponential phase physiology would be
334 prolonged in the Δ*acrB* mutant with σ^{70} remaining the dominant sigma factor. Oxygen limitation
335 caused by increased biomass concentration would likely activate FNR, which would upregulate the
336 anaerobic energy-generating pathways identified in group two above. Nrf, Nap and CCP do not
337 pump protons across the inner membrane (68), therefore they would not contribute to the

hyperpolarised state of the bacterium. ArcA does not appear to regulate the anaerobically-activated genes identified here in Supplemental Table S2 except for the periplasmic nitrite reductase *nrf* (62).

Experimental determination of membrane potential

To test whether the inner membrane of the Δ*acrB* strain is hyperpolarised, we used the ratiometric fluorescent membrane potential dye $DiOC_2(3)$ (3,3'-Diethyloxacarbocyanine Iodide). The wild type and Δ*acrB* strains were grown and the membrane potential measured using flow cytometry after 1, 3 and 5 hours (Figure 4a). As a control, the protonophore carbonyl cyanide m-chlorophenylhydrazone (CCCP) which collapses the PMF was used immediately prior to measurement. The wild type strain showed low membrane potential after 1 hour growth, and slightly higher after 3 hours and 5 hours. In each case, treatment with CCCP collapsed the membrane potential.

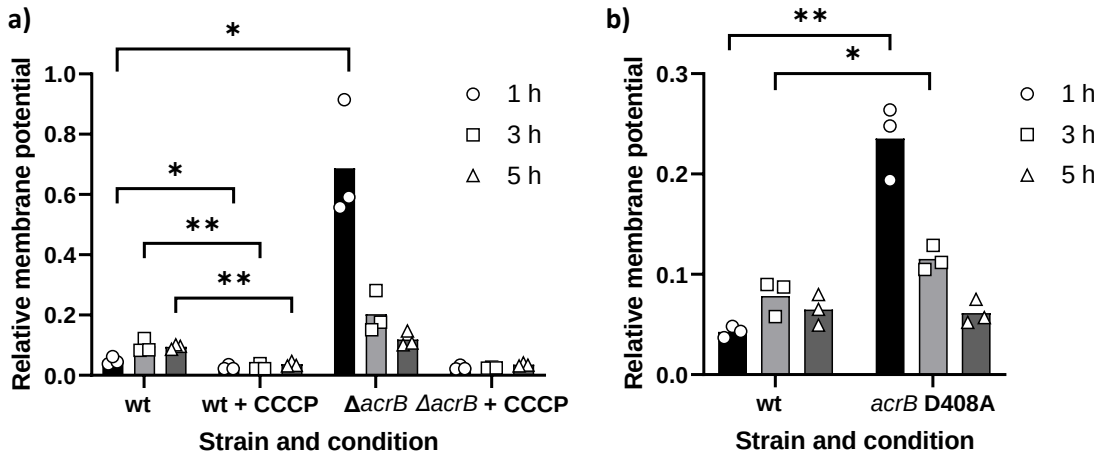

Figure 4. Determination of membrane potential. SL1344, Δ*acrB* and *acrB* D408A cells were grown in LB medium and samples taken at 1, 3 and 5 hours growth, whereupon membrane potential was determined using flow cytometry and $DiOC_2(3)$. The red/green fluorescence ratio, corresponding to membrane potential, is shown for each strain. The protonophore CCCP was used as a control to collapse membrane potential. (a) Comparison of wild type and *acrB* knockout; (b) comparison of wild type and *acrB* D408A mutant. Error bars show significance as determined using t test for selected comparisons; * $P < 0.05$; ** $P \leq 0.01$.

The Δ*acrB* mutant had far higher membrane potential than the wild type at 1 h, slightly higher at 3 h ($P = 0.064$), and comparable at 5 h growth. CCCP also collapsed the membrane potential in the Δ*acrB* strain. These data support the hypothesis that the Δ*acrB* mutant is hyperpolarised during rapid growth. This experiment was repeated with a strain harbouring a D408A mutation in *acrB*, which prevents proton translocation and thereby blocks efflux (69, 70). The *acrB* D408A mutation had comparable effects to the Δ*acrB* deletion on membrane potential (Figure 4b).

363 There is only one other study where the influence of efflux pumps on membrane potential has been
364 measured; Le *et al*. showed that PMF was similar in wt and *tolC* strains of *E. coli* by measuring
365 flagellar rotor speed (71). These experiments were done on cells grown in rich medium to an optical
366 density of 2. This is most comparable to our 5 hour timepoint, where membrane potential in wild
367 type and Δ*acrB* strains was similar.

368

369 **Discussion**

370 Our transcriptomics data suggests that the Δ*acrB* strain enters stationary phase later than the wild
371 type, and as a result displays prolonged exponential-phase anaerobic metabolism. Comparison with
372 other transcriptomic experiments on efflux pump mutants reveals some similarities in expression
373 patterns. Wang-Kan *et al*. compared expression in SL1344 and an efflux-defective *acrB* D408A
374 mutant (6). The two strains were grown in MOPS minimal medium to an OD_{600} of 0.6. The *acrB*
375 D408A mutant displayed higher expression of flagella and anaerobic metabolism genes than the wild
376 type. A later transcriptomic study (7) grew the same strains in LB broth to stationary phase and
377 found changes in genes responsible for energy metabolism. A major advantage of measuring gene
378 expression across growth (here at 1, 3 and 5 hours) is that trends in gene expression (and thereby
379 physiology) over time can be identified, which would otherwise be difficult to detect or interpret
380 when taking samples at only a single timepoint.

381 ***Supporting evidence for the redox-ArcBA model from the literature***

382 There is data in the literature to support the model of efflux pump function influencing membrane
383 potential and regulation of stationary phase (Fig. 3). The links between efflux pumps and membrane
384 potential have previously been observed in studies on efflux pump inhibitors. The antihistamine
385 promethazine (a phenothiazine) is an efflux pump inhibitor (72) and has been shown to increase
386 membrane potential in *Pseudomonas aeruginosa* (73).

387 Arce-Rodríguez *et al*. studied the impact of the $NADH:NAD^+$ ratio on antibiotic resistance in
388 *Pseudomonas aeruginosa* PA14 (74). They artificially modulated the $NADH:NAD^+$ ratio using a
389 recombinant NADH oxidase (which increases $[NAD^+]$) or a formate dehydrogenase (which increases
390 [NADH]). They showed that a high $NADH:NAD^+$ ratio increased membrane potential whereas low
391 $NADH:NAD^+$ ratios decreased membrane potential (measured using $DiOC_2(3)$). High $NADH:NAD^+$
392 ratios also increased cellular ROS levels, and efflux of aminoglycosides and fluoroquinolones via the
393 RND efflux pumps MexAB and MexXY leading to increased resistance. However, a high $NADH:NAD^+$
394 ratio also increased ROS-mediated killing by high concentrations of antibiotics, and it was concluded

395 that control of NADH:NAD^+ ratio and other aspects of redox balance was important for response to
396 antibiotics.

397 Yang *et al*. found that an Δ*acrA* mutant in *E. coli* BW25113 had lower *rpoS::lacZ* expression than the
398 wild type across growth, while overproduction of AcrA resulted in increased *rpoS::lacZ* expression
399 (75). Yang *et al*. proposed that efflux pumps export quorum sensing molecules which gives rise to
400 these changes in physiology, but we present an alternative model whereby membrane potential and
401 redox state is the signal. Indeed, subsequent studies have sought to identify effluxed quorum
402 sensing molecules without success (7). A previous study found that *rpoS* transcription in *S.*
403 Typhimurium F98 is linked to redox and influenced by oxygen, ArcA, and NADH:NAD^+ ratio (66).
404 Expression of *arcA* was also found to be negatively regulated by RpoS. The authors also suggested
405 that quorum sensing could play a role in this regulation. ArcA has also recently been found to be
406 important in *E. coli* for development of antibiotic resistance (76) and metabolic adaptation to
407 tetracycline resistance (77).

408 ***Links to biofilms?***

409 It has previously been reported that knockout or deactivation of *acrB* and other genes encoding
410 efflux pump components reduced biofilm formation in *Salmonella* (78), although the exact
411 regulatory mechanism is currently unclear (79, 80) . Indeed, efflux pumps have been implicated in
412 biofilm formation in many bacterial species (reviewed by (81)). A recent study identified TolC as
413 being beneficial for biofilm formation in both *E. coli* and *S*. Typhimurium (80). This study also
414 identified *nuo* genes encoding the major aerobic NADH reductase as being important in *Salmonella*
415 biofilm formation, and highlighted the fact that biofilm development is a process requiring different
416 genes at different times (from initial attachment to maturation). Efflux inhibitors such as
417 phenothiazines have also been shown to reduce biofilm formation (72, 73). ArcBA and RpoS have
418 previously been implicated in regulation of biofilm formation (82) so our model could provide a link
419 between efflux pumps, redox state, and biofilm formation. Indeed, recent studies have shown that
420 *Salmonella* biofilm formation can be modulated by redox-active polymers (83).

421

422 **Conclusions**

423 In summary, we have demonstrated that deactivation of AcrB leads to hyperpolarisation of the inner
424 membrane and we propose that this is responsible for wide-ranging changes in bacterial gene
425 regulation and physiology. Our model linking efflux and redox provides an explanation for some
426 phenotypes observed in efflux pump knockouts and inhibition experiments, and places efflux pumps

427 as a central part of bacterial physiology, distinct from (but linked to) their role as transporters of
428 noxious substances from the cell.

429 Intriguingly, our model could explain three reasons why efflux pumps are important for the response
430 of *Salmonella* to antimicrobials. First, their well-established and characterised function in removing
431 noxious substances from the cell. Second, as loss of AcrB function increases membrane potential,
432 antimicrobials postulated to function via the generation of reactive oxygen species by the
433 respiratory chain following treatment (the ROS-lethality hypothesis) (84) could be more effective.
434 And third, as the Δ*acrB* strain appears to enter stationary phase later in growth than the wild type,
435 inhibition of efflux is likely to delay the remodelling of the cell envelope that occurs on transition to
436 stationary phase, after which antimicrobial permeability is far reduced (9). Likewise, the attenuation
437 of virulence observed when AcrB is deactivated (6) could be due to deficiencies in efflux of
438 antimicrobial host molecules, and / or changes in physiology brought about by hyperpolarisation
439 such as alterations in SPI expression, motility, and biofilm formation. Future work will explore the
440 relative contributions of efflux and redox state in these situations.

441

442 **Materials and Methods**

443 *Salmonella enterica* serovar Typhimurium SL1344 (85) and its cognate Δ*acrB* (86) and *acrB* D408A
444 mutant (6) were used. Transcriptomic analysis on SL1344 and SL1344 Δ*acrB* was performed as
445 described by (9). RNA-Seq data have been deposited with Array Express (accession no. E-MTAB-
446 9679).

447 Total numbers of differentially expressed genes (DEGs) were determined using the R package DESeq2
448 (87) by comparing the three timepoints (1h, 3h, and 5h) for both the wild type and the Δ*acrB* strain.
449 Adjusted p-value < 0.05 and $\log_2$FC ≥ |1.5| were both used as the thresholds for determining the DEGs
450 for the Venn diagrams (Figure 1), which were drawn using the R package ggvenn (88).

451 Genes were classified in groups 1, 2 and 3 by the following criteria. The $\log_2$ fold change for each
452 gene was calculated for 1 h versus 3 h in both wt and Δ*acrB* strains. Only genes where $\log_2$FC data
453 were significant (p_{adj} < 0.05) for the 1 h vs 3 h comparison for both wt and Δ*acrB* strains were
454 considered for this analysis. Δ$\log_2$FC was calculated for each gene by subtracting the $\log_2$FC in the wt
455 from the $\log_2$FC in the Δ*acrB* strain. Groups were classified: group 1, wt $\log_2$FC for 1 h vs 3 h was ≤ -1
456 and Δ$\log_2$FC was ≥ 1; Group 2, wt $\log_2$FC for 1 h vs 3 h was > -1 and Δ$\log_2$FC was ≥ 1; Group 3, Δ$\log_2$FC
457 was ≤ 1.

458

459 **Membrane potential measurement by flow cytometry**

460 Strains SL1344, Δ*acrB* and *arcB* D408A were grown in 5 mL of Lennox broth (LB). After 1, 3 and 5
461 hours, cells were harvested by centrifugation (4720 x g for 5 min) and diluted in filter-sterilised
462 HEPES-buffered saline (HBS, Alfa Aesar). Diluted cell suspensions were added to 1.5 mL microfuge
463 tubes containing HBS and 3,3'-diethyloxacarbocyanine iodide ($DiOC_2(3)$, Invitrogen), with or without
464 carbonyl cyanide 3-chlorophenylhydrazone (CCCP, Acros Organics) as appropriate. $DiOC_2(3)$ and
465 CCCP were added to a final concentration of 30 µM and 15 µM respectively. Samples were incubated
466 in the dark at room temperature for 30 minutes before data were acquired. Unstained controls were
467 included for each strain alongside HBS-only controls. $DiOC_2(3)$ was prepared as a 3 mM stock in
468 dimethyl sulfoxide and CCCP was prepared as a 10 mM stock in 80% DMSO. Both were stored as
469 aliquots at -20 °C protected from light.

470 Data were acquired using an Attune® NxT Focusing Cytometer equipped with blue (488 nm) and
471 yellow (585 nm) lasers and the Attune® NxT software (ThermoFisher Scientific). Initial placement of
472 the sample acquisition gate (R1) was guided by SYTO-84 ™ (Invitrogen) staining of control samples.
473 SYTO-84 ™, prepared as per (89) was used at a final concentration of 10 µM to differentiate bacteria
474 from acellular particles. Event acquisition was set to 10,000 events in the R1 gate for stained
475 samples, or to 10,000 total events for unstained samples. Forward scatter (FSC-H) and side scatter
476 (SSC-H) voltages were set at 700 and 500 respectively. Blue laser (BL-1 and BL-3) voltages were each
477 set at 400. The draw volume (50 µL), flow rate (12.5 µL/min) and threshold (default) were defined.
478 Green and red fluorescence of $DiOC_2(3)$ was measured using the BL-1 (530/30 filter) and BL-3
479 (695/40 filter) channels respectively.

480 Compensation was applied for each experiment using cells harvested at 1 h. For the unstained
481 control, the wild type strain (SL1344) was suspended in filter sterilised HBS. For BL-1 and BL-3 laser
482 controls, $DiOC_2(3)$ and CCCP were included at final concentrations of 30 µM and 15 µM respectively
483 to replicate experimental conditions. Samples were vortexed thoroughly immediately before data
484 acquisition, and sip sanitisation was used between samples to minimise carryover. Calibration beads
485 (Attune Performance Tracking Beads, ThermoFisher Scientific) were used to ensure inter-
486 experimental consistency. FlowJo version 10.7.1 was used for data analysis.

487

488 **Acknowledgements**

489 ***Conflicts of interest:*** We declare that the research was conducted in the absence of any commercial
490 or financial relationships that might be considered a conflict of interest.

491 ***Author contributions:*** JMAB, TWO, and EEW designed the assays. EEW performed experiments to
492 obtain samples for RNA-seq. SJE performed experiments to measure membrane potential and
493 analysed the resulting data. RNA-seq data were analysed by EEW, OO, and TWO. The manuscript
494 was written by JMAB and TWO with input from all authors.

495 ***Funding:*** EEW was funded by AAMR Wellcome Trust DTP grant 108876/B/15/Z at the University of
496 Birmingham. OO was funded by a UK Biotechnology & Biological Sciences Research Council (BBSRC)
497 PhD studentship through the Midlands Integrative Biosciences Training Partnership (MIBTP) scheme.
498 SJE was funded by a Centre for Systems Modelling and Quantitative Biomedicine (SMQB), University
499 of Birmingham grant to JMAB. JMAB was funded by BBSRC grant BB/M02623X/1 (David Phillips
500 Fellowship to JMAB).

501 The authors would like to thank Xuan Wang-Kan and Laura Piddock for sharing data from previous
502 studies.

503

504 **References**

505 1. Darby EM, Trampari E, Siasat P, Gaya MS, Alav I, Webber MA, Blair JMA. 2022. Molecular
506 mechanisms of antibiotic resistance revisited. Nat Rev Microbiol
507 https://doi.org/10.1038/s41579-022-00820-y.

508 2. Blair JMA, Richmond GE, Piddock LJV. 2014. Multidrug efflux pumps in Gram-negative bacteria
509 and their role in antibiotic resistance. Future Microbiol 9:1165–1177.

510 3. Nikaido H. 1989. Outer membrane barrier as a mechanism of antimicrobial resistance.
511 Antimicrob Agents Chemother 33:1831–1836.

512 4. Colclough AL, Alav I, Whittle EE, Pugh HL, Darby EM, Legood SW, McNeil HE, Blair JMA. 2020.
513 RND efflux pumps in Gram-negative bacteria; Regulation, structure and role in antibiotic
514 resistance. Future Microbiol https://doi.org/10.2217/fmb-2019-0235.

515 5. Webber MA, Bailey AM, Blair JMA, Morgan E, Stevens MP, Hinton JCD, Ivens A, Wain J,
516 Piddock LJV. 2009. The global consequence of disruption of the AcrAB-TolC efflux pump in
517 *Salmonella enterica* includes reduced expression of SPI-1 and other attributes required to
518 infect the host. J Bacteriol 191:4276–4285.

519 6. Wang-Kan X, Blair JMA, Chirullo B, Betts J, La Ragione RM, Ivens A, Ricci V, Opperman TJ,
520 Piddock LJV. 2017. Lack of AcrB efflux function confers loss of virulence on *Salmonella enterica*
521 serovar Typhimurium. MBio 8:e00968-17.

522 7. Wang-Kan X, Rodríguez-Blanco G, Southam AD, Winder CL, Dunn WB, Ivens A, Piddock LJV.
523 2021. Metabolomics reveal potential natural substrates of *acrB* in *Escherichia coli* and
524 *Salmonella enterica* serovar Typhimurium. MBio 12:e00109-21.

525 8. Buckner MMC, Blair JMA, La Ragione RM, Newcombe J, Dwyer DJ, Ivens A, Piddock LJV. 2016.
526 Beyond antimicrobial resistance: Evidence for a distinct role of the AcrD efflux pump in
527 *Salmonella* biology. MBio 7:e01916-16.

528 9. Whittle EE, McNeil HE, Trampari E, Webber M, Overton TW, Blair JMA. 2021. Efflux Impacts
529 Intracellular Accumulation Only in Actively Growing Bacterial Cells. MBio 12:e0260821.

530 10. Leus I V., Adamiak J, Chandar B, Bonifay V, Zhao S, Walker SS, Squadroni B, Balibar CJ,
531 Kinarivala N, Standke LC, Voss HU, Tan DS, Rybenkov V V., Zgurskaya HI. 2023. Functional
532 Diversity of Gram-Negative Permeability Barriers Reflected in Antibacterial Activities and
533 Intracellular Accumulation of Antibiotics. Antimicrob Agents Chemother 67:e01377-22.

534 11. Manrique PD, López CA, Gnanakaran S, Rybenkov V V., Zgurskaya HI. 2023. New
535 understanding of multidrug efflux and permeation in antibiotic resistance, persistence, and
536 heteroresistance. Ann N Y Acad Sci 1519:46–62.

537 12. Li J, Claudi B, Fanous J, Chicherova N, Cianfanelli FR, Campbell RAA, Bumann D. 2021. Tissue
538 compartmentalization enables *Salmonella* persistence during chemotherapy. Proc Natl Acad
539 Sci U S A 118:e2113951118.

540 13. Łapińska U, Voliotis M, Lee KK, Campey A, Stone RML, Tuck B, Phetsang W, Zhang B, Tsaneva-
541 Atanasova K, Blaskovich MAT, Pagliara S. 2022. Fast bacterial growth reduces antibiotic
542 accumulation and efficacy. Elife 11:e74062.

543 14. Navarro Llorens JM, Tormo A, Martínez-García E. 2010. Stationary phase in Gram-negative
544 bacteria. FEMS Microbiol Rev 34:476–495.

545 15. Battesti A, Majdalani N, Gottesman S. 2011. The RpoS-mediated general stress response in
546 *Escherichia coli* . Annu Rev Microbiol 65:189–213.

547 16. Durfee T, Hansen AM, Zhi H, Blattner FR, Ding JJ. 2008. Transcription profiling of the stringent
548 response in *Escherichia coli*. J Bacteriol 190:1084–1096.

549 17. Singh SK, Saisree L, Amrutha RN, Reddy M. 2012. Three redundant murein endopeptidases
550 catalyse an essential cleavage step in peptidoglycan synthesis of *Escherichia coli* K12. Mol
551 Microbiol 86:1036–1051.

552 18. Harmon DE, Ruiz C. 2022. The Multidrug Efflux Regulator AcrR of *Escherichia coli* Responds to
553 Exogenous and Endogenous Ligands To Regulate Efflux and Detoxification. mSphere 7:e00474-
554 22.

555 19. Lou L, Zhang P, Piao R, Wang Y. 2019. *Salmonella* Pathogenicity Island 1 (SPI-1) and Its
556 Complex Regulatory Network. Front Cell Infect Microbiol 9:270

557 20. Sánchez-Romero MA, Casadesús J. 2018. Contribution of SPI-1 bistability to *Salmonella*
558 *enterica* cooperative virulence: insights from single cell analysis. Sci Rep 8:14875.

559 21. Ilyas B, Tsai CN, Coombes BK. 2017. Evolution of *Salmonella*-host cell interactions through a
560 dynamic bacterial genome. Front Cell Infect Microbiol 7:428.

561 22. Kröger C, Colgan A, Srikumar S, Händler K, Sivasankaran SK, Hammarlöf DL, Canals R, Grissom
562 JE, Conway T, Hokamp K, Hinton JCD. 2013. An infection-relevant transcriptomic compendium
563 for *Salmonella enterica* serovar Typhimurium. Cell Host Microbe 14:683–695.

564 23. Srikumar S, Kröger C, Hébrard M, Colgan A, Owen S V., Sivasankaran SK, Cameron ADS,
565 Hokamp K, Hinton JCD. 2015. RNA-seq Brings New Insights to the Intra-Macrophage
566 Transcriptome of *Salmonella* Typhimurium. PLoS Pathog 11:e1005262.

567 24. Hoiseth SK, Stocker BAD. 1981. Aromatic-dependent *Salmonella* Typhimurium are non-
568 virulent and effective as live vaccines. Nature 291:238–239.

569 25. Fink RC, Evans MR, Porwollik S, Vazquez-Torres A, Jones-Carson J, Troxell B, Libby SJ,
570 McClelland M, Hassan HM. 2007. FNR is a global regulator of virulence and anaerobic
571 metabolism in *Salmonella enterica* serovar Typhimurium (ATCC 14028s). J Bacteriol 189:2262–
572 2273.

573 26. Constantinidou C, Hobman JL, Griffiths L, Patel MD, Penn CW, Cole JA, Overton TW. 2006. A
574 reassessment of the FNR regulon and transcriptomic analysis of the effects of nitrate, nitrite,
575 NarXL, and NarQP as *Escherichia coli* K12 adapts from aerobic to anaerobic growth. J Biol
576 Chem 281:4802–4815.

577 27. Nilavongse A, Brondijk THC, Overton TW, Richardson DJ, Leach ER, Cole JA. 2006. The NapF
578 protein of the *Escherichia coli* periplasmic nitrate reductase system: Demonstration of a
579 cytoplasmic location and interaction with the catalytic subunit, NapA. Microbiology 152:3227–
580 3237.

581 28. Browning DF, Grainger DC, Beatty CM, Wolfe AJ, Cole JA, Busby SJW. 2005. Integration of
582 three signals at the *Escherichia coli nrf* promoter: A role for Fis protein in catabolite
583 repression. Mol Microbiol 57:496–510.

584 29. Kim MJ, Lim S, Ryu S. 2008. Molecular analysis of the *Salmonella* Typhimurium *tdc* operon
585 regulation. J Microbiol Biotechnol 18:1024–1032.

586 30. Cianciotto NP, Cornelis P, Baysse C. 2005. Impact of the bacterial type I cytochrome *c*
587 maturation system on different biological processes. Mol Microbiol 56:1408–1415.

588 31. Khademian M, Imlay JA. 2017. *Escherichia coli* cytochrome *c* peroxidase is a respiratory
589 oxidase that enables the use of hydrogen peroxide as a terminal electron acceptor. Proc Natl
590 Acad Sci U S A 114:E6922–E6931.

591 32. Pelosi L, Vo CDT, Abby SS, Loiseau L, Rascalou B, Chehade MH, Faivre B, Goussé M, Chenal C,
592 Touati N, Binet L, Cornu D, Fyfe CD, Fontecave M, Barras F, Lombard M, Pierrel F. 2019.
593 Ubiquinone biosynthesis over the entire O_2 range: Characterization of a conserved O_2-
594 independent pathway. MBio 10:e01319-19.

595 33. Navarro C, Wu L -F, Mandrand-Berthelot M -A. 1993. The *nik* operon of *Escherichia coli*
596 encodes a periplasmic binding-protein-dependent transport system for nickel. Mol Microbiol
597 9:1181–1191.

598 34. Rowe JL, Starnes GL, Chivers PT. 2005. Complex transcriptional control links NikABCDE-
599 dependent nickel transport with hydrogenase expression in *Escherichia coli*. J Bacteriol
600 187:6317–6323.

601 35. Piotrowska AA. 2018. PhD thesis. Investigation of STM3071 as a potential regulator of cobalt
602 transport in *Salmonella enterica.* Edinburgh Napier University, Edinburgh, Scotland.

603 36. Karavolos MH, Spencer H, Bulmer DM, Thompson A, Winzer K, Williams P, Hinton JCD, Khan
604 CMA. 2008. Adrenaline modulates the global transcriptional profile of *Salmonella* revealing a

605 role in the antimicrobial peptide and oxidative stress resistance responses. BMC Genomics
606 9:458.

607 37. Wood MW, Jones MA, Watson PR, Hedges S, Wallis TS, Galyov EE. 1998. Identification of a
608 pathogenicity island required for *Salmonella* enteropathogenicity. Mol Microbiol 29:883–891.

609 38. Cohen H, Adani B, Cohen E, Piscon B, Azriel S, Desai P, Bähre H, McClelland M, Rahav G, Gal-
610 Mor O. 2022. The ancestral stringent response potentiator, DksA has been adapted
611 throughout *Salmonella* evolution to orchestrate the expression of metabolic, motility, and
612 virulence pathways. Gut Microbes 14:1997294.

613 39. Frye J, Karlinsey JE, Felise HR, Marzolf B, Dowidar N, McClelland M, Hughes KT. 2006.
614 Identification of new flagellar genes of *Salmonella enterica* serovar Typhimurium. J Bacteriol
615 188:2233–2243.

616 40. Hamed S, Wang X, Shawky RM, Emara M, Aldridge PD, Rao C V. 2019. Synergistic action of SPI-
617 1 gene expression in *Salmonella enterica* serovar Typhimurium through transcriptional
618 crosstalk with the flagellar system. BMC Microbiol 19:211.

619 41. Liu R, Blackwell TW, States DJ. 2001. Conformational model for binding site recognition by the
620 *E. coli* MetJ transcription factor. Bioinformatics 17:622–633.

621 42. Grogan DW, Cronan JE. 1997. Cyclopropane ring formation in membrane lipids of bacteria.
622 Microbiol Mol Biol Rev 61:429–441.

623 43. Wei Y, Newman EB. 2002. Studies on the role of the *metK* gene product of *Escherichia coli* K-
624 12. Mol Microbiol 43:1651–1656.

625 44. Newman EB, Budman LI, Chan EC, Greene RC, Lin RT, Woldringh CL, D'ari R. 1998. Lack of S-
626 adenosylmethionine results in a cell division defect in *Escherichia coli*. J Bacteriol 180:3614–
627 3619.

628 45. Husna AU, Wang N, Cobbold SA, Newton HJ, Hocking DM, Wilksch JJ, Scott TA, Davies MR,
629 Hinton JC, Tree JJ, Lithgow T, McConville MJ, Strugnell RA. 2018. Methionine biosynthesis and
630 transport are functionally redundant for the growth and virulence of *Salmonella* Typhimurium.
631 J Biol Chem 293:9506–9519.

632 46. Zimbro MJ, Power DA, Miller SM, Wilson GE, Johnson JA. 2009. Difco and BBL Manual.

633 47. Dolzan M, Johansson K, Roig-Zamboni V, Campanacci V, Tegoni M, Schneider G, Cambillau C.
634 2004. Crystal structure and reactivity of YbdL from *Escherichia coli* identify a methionine
635 aminotransferase function. FEBS Lett 571:141–146.

636 48. Heilbronn J, Wilson J, Berger BJ. 1999. Tyrosine aminotransferase catalyzes the final step of
637 methionine recycling in *Klebsiella pneumoniae*. J Bacteriol 181:1739–1747.

638 49. Sévin DC, Fuhrer T, Zamboni N, Sauer U. 2017. Nontargeted in vitro metabolomics for high-
639 throughput identification of novel enzymes in *Escherichia coli*. Nat Methods 14:187–194.

640 50. Hwang S, Choe D, Yoo M, Cho S, Kim SC, Cho S, Cho BK. 2018. Peptide transporter CstA
641 imports pyruvate in *Escherichia coli* K-12. J Bacteriol 200:e00771-17.

642 51. McDermott JE, Yoon H, Nakayasu ES, Metz TO, Hyduke DR, Kidwai AS, Palsson BO, Adkins JN,
643 Heffron F. 2011. Technologies and approaches to elucidate and model the virulence program
644 of *Salmonella*. Front Microbiol 2:121.

645 52. Taschner NP, Yagil E, Spira B. 2004. A differential effect of σ^S on the expression of the Pho
646 regulon genes of *Escherichia coli*. Microbiology 150:2985–2992.

647 53. Typas A, Stella S, Johnson RC, Hengge R. 2007. The -35 sequence location and the Fis-sigma
648 factor interface determine σ^S selectivity of the *proP* (P2) promoter in *Escherichia coli*. Mol
649 Microbiol 63:780–796.

650 54. Weber H, Polen T, Heuveling J, Wendisch VF, Hengge R. 2005. Genome-wide analysis of the
651 general stress response network in *Escherichia coli*: σ^S-dependent genes, promoters, and
652 sigma factor selectivity. J Bacteriol 187:1591–1603.

653 55. Mukhopadhyay S, Schellhorn HE. 1994. Induction of *Escherichia coli* hydroperoxidase I by
654 acetate and other weak acids. J Bacteriol 176:2300–2307.

655 56. Piper SE, Mitchell JE, Lee DJ, Busby SJW. 2009. A global view of *Escherichia coli* Rsd protein and
656 its interactions. Mol Biosyst 5:1943–1947.

657 57. Starosta AL, Lassak J, Jung K, Wilson DN. 2014. The bacterial translation stress response. FEMS
658 Microbiol Rev 38:1172–1201.

659 58. Waegeman H, Beauprez J, Moens H, Maertens J, De Mey M, Foulquié-Moreno MR, Heijnen JJ,
660 Charlier D, Soetaert W. 2011. Effect of *iclR* and *arcA* knockouts on biomass formation and
661 metabolic fluxes in *Escherichia coli* K12 and its implications on understanding the metabolism
662 of *Escherichia coli* BL21 (DE3). BMC Microbiol 11:70.

663 59. Brown AN, Anderson MT, Bachman MA, Mobley HLT. 2022. The ArcAB Two-Component
664 System: Function in Metabolism, Redox Control, and Infection. Microbiol Mol Biol Rev
665 86:e0011021.

666 60. Pardo-Esté C, Hidalgo AA, Aguirre C, Briones AC, Cabezas CE, Castro-Severyn J, Fuentes JA,
667 Opazo CM, Riedel CA, Otero C, Pacheco R, Valvano MA, Saavedra CP. 2018. The ArcAB two-
668 component regulatory system promotes resistance to reactive oxygen species and systemic
669 infection by *Salmonella* Typhimurium. PLoS One 13:e0203497.

670 61. Morales EH, Collao B, Desai PT, Calderón IL, Gil F, Luraschi R, Porwollik S, McClelland M,
671 Saavedra CP. 2013. Probing the ArcA regulon under aerobic/ROS conditions in *Salmonella*
672 *enterica* serovar Typhimurium. BMC Genomics 14:626.

673 62. Evans MR, Fink RC, Vazquez-Torres A, Porwollik S, Jones-Carson J, McClelland M, Hassan HM.
674 2011. Analysis of the ArcA regulon in anaerobically grown *Salmonella enterica* sv.
675 Typhimurium. BMC Microbiol 11:58.

676 63. Sharma P, Stagge S, Bekker M, Bettenbrock K, Hellingwerf KJ. 2013. Kinase Activity of ArcB
677 from *Escherichia coli* Is Subject to Regulation by Both Ubiquinone and Demethylmenaquinone.
678 PLoS One 8:e75412.

679 64. Yoshida H, Wada A, Shimada T, Maki Y, Ishihama A. 2019. Coordinated Regulation of Rsd and
680 RMF for Simultaneous Hibernation of Transcription Apparatus and Translation Machinery in
681 Stationary-Phase *Escherichia coli*. Front Genet 10:1153.

682 65. Mika F, Hengge R. 2005. A two-component phosphotransfer network involving ArcB, ArcA, and
683 RssB coordinates synthesis and proteolysis of σS (RpoS) in E. coli. Genes Dev 19:2770–2781.

684 66. Ševčík M, Šebková A, Volf J, Rychlík I. 2001. Transcription of *arcA* and *rpoS* during growth of
685 *Salmonella* Typhimurium under aerobic and microaerobic conditions. Microbiology 147:701–
686 708.

687 67. Park DM, Akhtar MS, Ansari AZ, Landick R, Kiley PJ. 2013. The Bacterial Response Regulator
688 ArcA Uses a Diverse Binding Site Architecture to Regulate Carbon Oxidation Globally. PLoS
689 Genet 9:e1003839.

690 68. Simon J, van Spanning RJM, Richardson DJ. 2008. The organisation of proton motive and non-
691 proton motive redox loops in prokaryotic respiratory systems. Biochim Biophys Acta -
692 Bioenerg 1777:1480–1490.

693 69. Seeger MA, Von Ballmoos C, Verrey F, Pos KM. 2009. Crucial role of Asp408 in the proton
694 translocation pathway of multidrug transporter AcrB: Evidence from site-directed mutagenesis
695 and carbodiimide labeling. Biochemistry 48:5801–5812.

696 70. Su CC, Li M, Gu R, Takatsuka Y, McDermott G, Nikaido H, Yu EW. 2006. Conformation of the
697 AcrB multidrug efflux pump in mutants of the putative proton relay pathway. J Bacteriol
698 188:7290–7296.

699 71. Le D, Krasnopeeva E, Sinjab F, Pilizota T, Kim M. 2021. Active efflux leads to heterogeneous
700 dissipation of proton motive force by protonophores in bacteria. MBio 12:e0067621.

701 72. Grimsey EM, Piddock LJV. 2019. Do phenothiazines possess antimicrobial and efflux inhibitory
702 properties? FEMS Microbiol Rev 43:577–590.

703 73. Donnert M, Elsheikh S, Arce-Rodriguez A, Pawar V, Braubach P, Jonigk D, Haverich A, Weiss S,
704 Müsken M, Häussler S. 2020. Targeting bioenergetics is key to counteracting the drug-tolerant
705 state of biofilm-grown bacteria. PLoS Pathog 16:e1009126.

706 74. Arce-Rodríguez A, Pankratz D, Preusse M, Nikel PI, Häussler S. 2022. Dual Effect: High NADH
707 Levels Contribute to Efflux-Mediated Antibiotic Resistance but Drive Lethality Mediated by
708 Reactive Oxygen Species. MBio 13:e0243421.

709 75. Yang S, Lopez CR, Zechiedrich EL. 2006. Quorum sensing and multidrug transporters in
710 *Escherichia coli*. Proc Natl Acad Sci U S A 103:2386–2391.

711 76. Horinouchi T, Maeda T, Kotani H, Furusawa C. 2020. Suppression of antibiotic resistance
712 evolution by single-gene deletion. Sci Rep 10:4178.

713 77. Arrieta-Ortiz ML, Pan M, Kaur A, Pepper-Tunick E, Srinivas V, Dash A, Immanuel SRC, Brooks
714 AN, Shepherd TR, Baliga NS. 2023. Disrupting the ArcA Regulatory Network Amplifies the
715 Fitness Cost of Tetracycline Resistance in *Escherichia coli*. mSystems 8:e00904-22.

716 78. Baugh S, Ekanayaka AS, Piddock LJV, Webber MA. 2012. Loss of or inhibition of all multidrug
717 resistance efflux pumps of *Salmonella enterica* serovar Typhimurium results in impaired ability
718 to form a biofilm. J Antimicrob Chemother 67:2409–2417.

719 79. Holden ER, Webber MA. 2020. MarA, RamA, and SoxS as Mediators of the Stress Response:
720 Survival at a Cost. Front Microbiol 11:828.

721 80. Holden ER, Yasir M, Turner AK, Charles IG, Webber MA. 2022. Comparison of the genetic basis
722 of biofilm formation between *Salmonella* Typhimurium and *Escherichia coli*. Microb Genomics
723 8:000885.

724 81. Alav I, Sutton JM, Rahman KM. 2018. Role of bacterial efflux pumps in biofilm formation. J
725 Antimicrob Chemother 73:2003–2020.

726 82. Hengge R. 2008. The two-component network and the general stress sigma factor RpoS (σ^S) in
727 *Escherichia coli*. Adv Exp Med Biol 631:40–53.

728 83. Gomez-Carretero S, Libberton B, Svennersten K, Persson K, Jager E, Berggren M, Rhen M,
729 Richter-Dahlfors A. 2017. Redox-active conducting polymers modulate *Salmonella* biofilm
730 formation by controlling availability of electron acceptors. npj Biofilms Microbiomes 3:19.

731 84. Kohanski MA, Dwyer DJ, Hayete B, Lawrence CA, Collins JJ. 2007. A Common Mechanism of
732 Cellular Death Induced by Bactericidal Antibiotics. Cell 130:797–810.

733 85. Brenner FW, Villar RG, Angulo FJ, Tauxe R, Swaminathan B. 2000. *Salmonella* nomenclature. J
734 Clin Microbiol 38:2465–2467.

735 86. Eaves DJ, Ricci V, Piddock LJV. 2004. Expression of *acrB, acrF, acrD, marA,* and *soxS* in
736 *Salmonella enterica* Serovar Typhimurium: Role in Multiple Antibiotic Resistance. Antimicrob
737 Agents Chemother 48:1145–1150.

738 87. Love MI, Huber W, Anders S. 2014. Moderated estimation of fold change and dispersion for
739 RNA-seq data with DESeq2. Genome Biol 15:550.

740 88. Gao CH, Yu G, Cai P. 2021. ggVennDiagram: An Intuitive, Easy-to-Use, and Highly Customizable
741 R Package to Generate Venn Diagram. Front Genet 12:706907.

742 89. Whittle EE, Legood SW, Alav I, Dulyayangkul P, Overton TW, Blair JMA. 2019. Flow Cytometric
743 Analysis of Efflux by Dye Accumulation. Front Microbiol 10:2319.

744